



# Newsletter

May 2001

## Introduction/Status

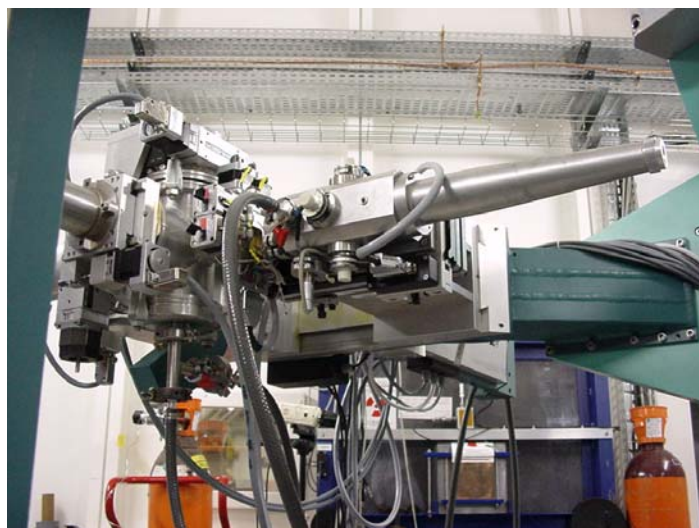
The XMaS beamline has just entered its 4th year of user operation and interest in it continues unabated. In the last proposal round there was a healthy over-subscription as, in previous rounds. There is also



*A view of the new low temperature ( $>1.8K$ ) sample environment in operation on a recent user experiment. Also in the view, behind the Be dome of the cryostat, is the "tube slit" assembly. Both facilities have seen service in several user experiments.*

growing interest in XMaS from ESRF users generally, with a full quota of ESRF experiments being scheduled.

In previous issues of the Newsletter we have described new facility upgrades that had either been introduced or were imminent. On this page we show some of the more recent additions in routine use. Overleaf is shown a set of data from an experiment which has benefited from the use of the new tube slits, together with reports of other activities. Subsequent pages contain brief examples of just a few of the experiments carried out by users during the past 12 months.



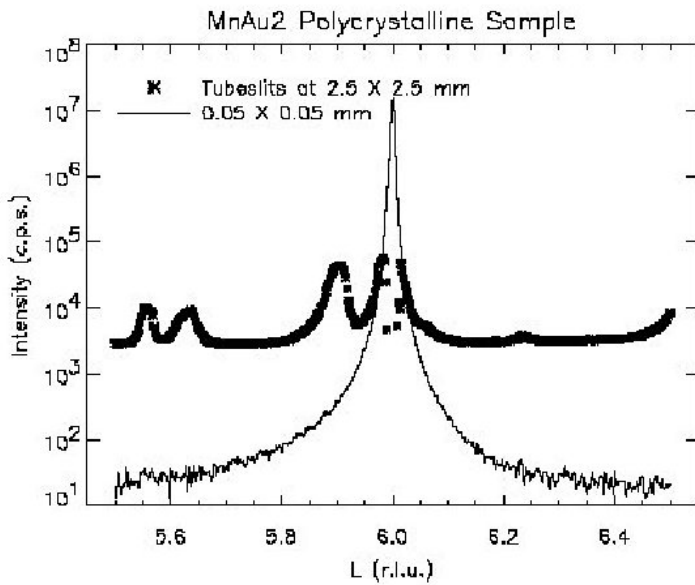
*Another view showing the tube slit assembly mounted on the detector arm of the diffractometer. Performance data is presented on the following page, with the slits, in this case, mounted just upstream of the sample.*



THE UNIVERSITY  
of LIVERPOOL

 *is an EPSRC sponsored project*

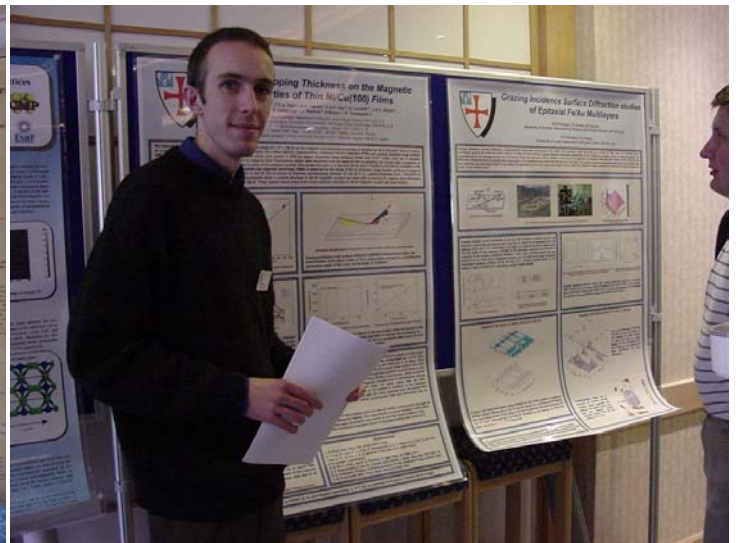




These data, taken during a recent user experiment, show an important aspect of the performance of the tube slits. The sample was polycrystalline and the curve representing the data collected using the large slit opening is a powder pattern. With the very fine slit setting Steve Collins and Dave Laundry were able to define a single crystallite and the single crystal peak (6 orders above background) resulted.



The phase plate assembly being commissioned. A brief report of a commissioning experiment is included among the reports of experiments featured on the pages that follow. When not in use the crystal holder can be demounted to allow beam access or, if necessary, the complete assembly can be easily removed.



The two photographs above were taken during the poster session of the XMaS Workshop, held at Warwick University in October 2000. The theme of the workshop was the further development of the beamline, both for the remainder of the current 5 year contract, and beyond. The aim was to involve XMaS users in the choices for further instrumental developments based upon their perceived requirements for the science they wish to investigate. The workshop was well attended and the XMaS team wish to thank all the participants, especially those who presented talks and displayed posters. There was lively discussion and helpful suggestions were made as to how the beamline should develop. Progress on XMaS was summarised and analysed by Gerry Lander and Paul Fewster. Following this meeting the Project Management Committee, established three working "focus" groups to investigate and make recommendations about possible upgrades under the headings: sample environment; detectors—especially 2-d; monochromator upgrades. A variety of initiatives are being pursued with eventual upgrades in mind.



# Some Recent Experiments

## Two growth modes of holmium: a transition through the critical thickness

*M. J. Bentall, R. A. Cowley, A. Yu. Babkevich, R. C. C. Ward, M. R. Wells, A. Stunault - for further information contact R. A. Cowley at Oxford Physics, Clarendon Laboratory, Parks Road, Oxford OX1 3PU r.cowley@physics.ox.ac.uk*

A series of high quality single crystal thin films of holmium staircase structures grown on thick yttrium seeds have been prepared at Oxford using molecular beam epitaxy techniques. The structure of these thin films has been studied by high-resolution x-ray diffraction both at the XMaS beamline at the ESRF and also with in-house facilities at Oxford.

Due to the lattice mismatch between the thin film and the seed theory suggests that the holmium layer is lattice-matched to the yttrium substrate for thicknesses less than a critical thickness,  $h_c$ . For thicker films it is energetically favourable for the spontaneous creation of dislocations to relieve the misfit strain in the basal plane. Further increases in the thickness lead to increasing numbers of dislocations and to the holmium film in-plane lattice parameter tending to the corresponding lattice parameter of bulk holmium.

X-ray scattering measurements of the (-10·5) Bragg reflection allowed the in-plane strain to be obtained as a function of holmium thickness, see Figure 1. Below  $\sim 125$  Å the holmium layer is highly strained because it is lattice-matched to the yttrium substrate. Above  $\sim 125$  Å, some of the strain is relieved by the introduction of misfit dislocations into the holmium layer. Above 700 Å, the strain tends asymptotically towards the value (0.019) that would be expected from the bulk lattice parameters of holmium and yttrium.

X-ray scattering measurements around the (002), (004) and (006) Bragg reflections allowed the out-of-plane strain to be determined and produced the transverse peak shapes shown in Figure 2. For holmium films thicker than  $\sim 125$  Å, the two-component line shapes show that misfit dislocations have partially relaxed the strain. This corresponds to the region of large in-plane strain with respect to the yttrium, highlighted by the red arrow in Figure 1. Below  $\sim 125$  Å the holmium peak shape closely resembles the yttrium peak shape, showing that the layer grows pseudomorphically and is lattice matched to the yttrium substrate. Here the holmium film is highly strained, and so its in-plane strain with respect to the yttrium layer is small. The black arrow in Figure 1 marks this region.

These results show that the critical thickness at which misfit dislocations begin to set in is  $(125\pm 20)$  Å for holmium grown on thick yttrium. It is the transition point between pseudomorphic film growth and dislocated film growth. This result is in disagreement with the theoretical prediction of a critical thickness of 40 Å.

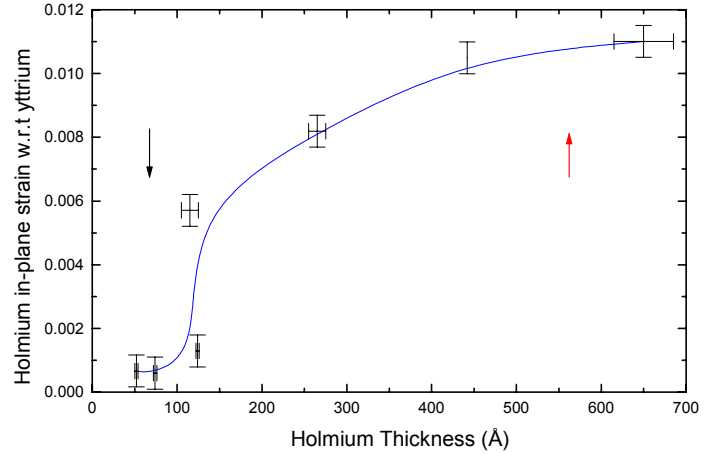


Figure 1: In-plane strain calculated from off-axis peaks with respect to the yttrium substrate.

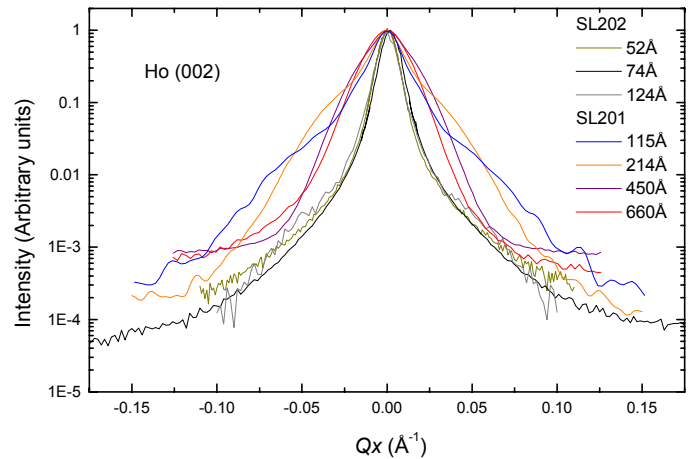


Figure 2: Transverse scans through (002) holmium. The change in lineshape of the holmium peak shows the transition from pseudomorphic, undislocated film growth below 125 Å to dislocated film growth for films above 125 Å.

## Study of magneto-elastic effects in a samarium film

*A. Stunault, K. Dumesnil, C. Dufour — for further information contact A. Stunault, I.L.L., Grenoble. stunault@ill.fr*

We have made extensive use of synchrotron X-ray magnetic and charge scattering to study the temperature dependence of long-range magnetic order in samarium, and of the related magneto-elastic effects. The sample was a samarium 5000 Å epitaxial film, grown by MBE in the Laboratoire de Physique des Matériaux, University of Nancy. It was chosen for its good crystal quality: coherence length of the order of 800 Å along the growth direction  $c$ , and

mosaic spread  $0.13^\circ$ . The structural and magnetic properties are similar to those of bulk samarium and are summarized in Figure 1. Resonant magnetic scattering is shell selective and we could study the behaviour of the  $4f$  and  $5d$  electrons through the magnetic phase transitions separately, with the photon energy tuned close to the samarium  $L_3$  absorption edge. Simultaneously, we have followed the behaviour of strong charge reflections through the magnetic phase transitions. Figure 2 shows scans along  $c^*$  of the  $(0, 0, 18)$  reflection. The indexing uses the lattice constant at 9 K. The peak position jumps by  $\Delta L/L = 6 \cdot 10^{-4}$  at the phase transition, reflecting a similar change  $\Delta c/c$  in the lattice constant. This result is consistent with earlier measurements on bulk samarium. We also observed charge reflections of type  $(0, 0, 9n \pm 3)$ ,  $n$  integer. These reflections are allowed by space group symmetry, but would have zero intensity for equidistant Sm planes. We interpret these weak reflections in terms of deviations  $e$  of the inter-planar distances from the ideal value of  $c/9$  (Figure 1). The thermal evolution of the weak  $(0, 0, 15)$  and strong  $(0, 0, 18)$  reflections is shown in Figure 3. The dip in the  $(0, 0, 18)$  intensity is only an artifact related to the integration along  $c^*$  (see Figure 2). The comparison of the  $(0, 0, 15)$  and  $(0, 0, 18)$  intensities leads to displacements  $e$  of the order of  $4 \cdot 10^{-5} c$  to  $1.2 \cdot 10^{-4} c$ .

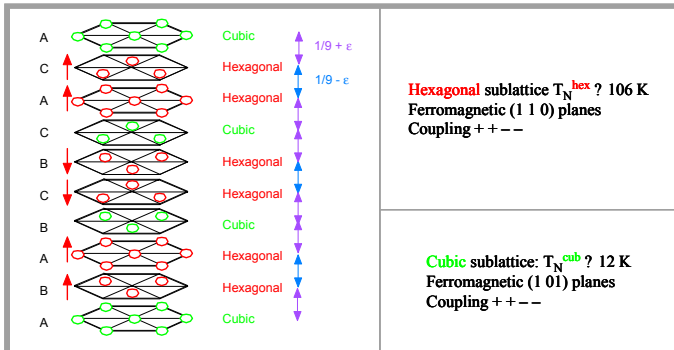


Figure 1 Crystal and magnetic structures of samarium. Model for magneto-elastic effects

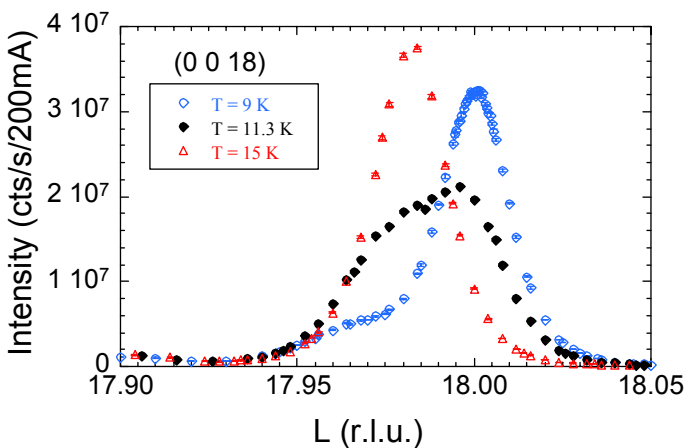


Figure 2 Magnetostriction on a macroscopic scale: the displacement of the  $(0, 0, 18)$  charge peak reflects an abrupt change in the  $c$  lattice constant at  $T_N^{\text{cub}}$

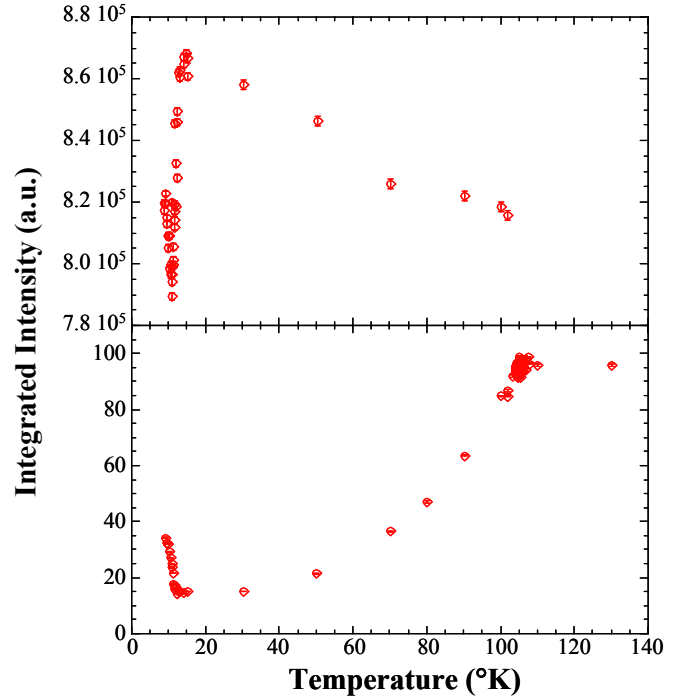


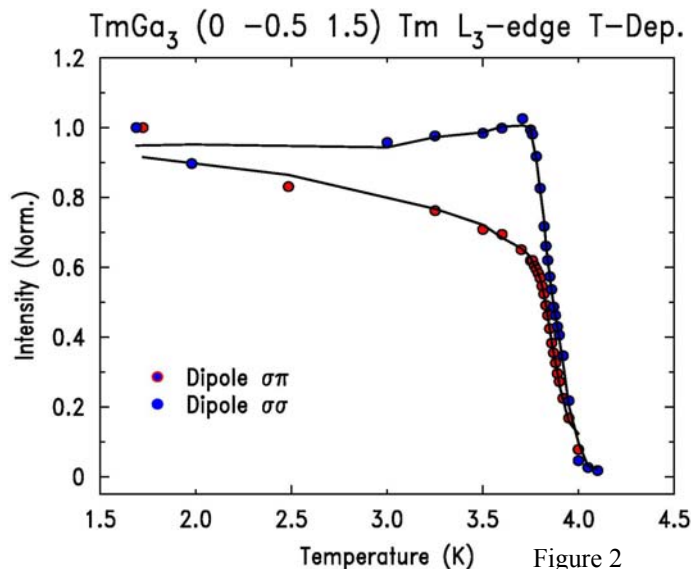
Figure 3 Thermal evolution of the weak  $(0, 0, 15)$  and strong  $(0, 0, 18)$  charge reflections, demonstrating magneto-elastic effects on a microscopic scale, at the level of inter-planar distances inside the unit cell.

## Interplay of Antiferromagnetism and Antiferroquadrupolar Ordering in $\text{TmGa}_3$

*D. Mannix, F. Yakhou, S.D. Brown, P. Thompson.—for further information contact D. Mannix XMaS BM28, ESRF, Grenoble danny@esrf.fr*

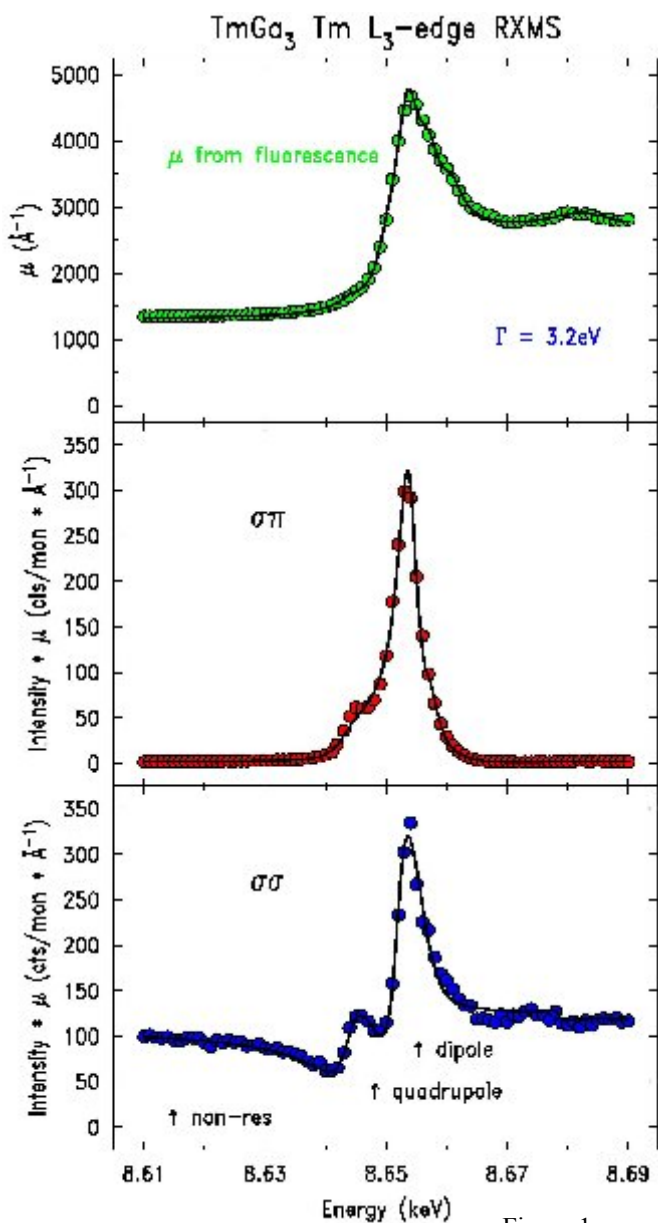
The spatial ordering of higher order multipoles of the lanthanide and actinide  $f$ -electron wavefunctions can be investigated directly by resonant x-ray scattering (neutrons do not directly couple to these  $f$ -electron quadrupolar interactions and so can only provide direct information on the magnetic bipolar ordering).  $\text{TmGa}_3$  undergoes a first order phase transition to an antiferroquadrupolar structure below  $T_Q = 4.29 \text{ K}$ , slightly before the onset of antiferromagnetism at  $T_N = 3.26 \text{ K}$ . We have investigated these two phases using x-ray resonant scattering at XMaS. The antiferroquadrupolar order and antiferromagnetism occur at the same propagation wavevector  $q = (0 \frac{1}{2} \frac{1}{2})$ , however, the scattering from magnetic bipoles and electric quadrupoles can be separated using polarisation analysis. The resonant scattering at the  $(0, 0.5, 1.5)$  position for  $\sigma\sigma$  (blue circles) and  $\sigma\pi$  (red circles), in the vicinity of the Tm  $L_3$  absorption edge, is shown in Figure 1. The green circles in the top panel are the absorption coefficients taken from the measured fluorescence. Since dipole resonant x-ray magnetic scattering is forbidden in the  $\sigma\sigma$  channel, the observation of such scattering arises purely from the antiferroquadrupolar ordering. The temperature

dependence of the dipole resonance of the  $\sigma\sigma$  and  $\sigma\pi$  intensities are compared in Figure 2. From the temperature dependence we ascribe the  $\sigma\pi$  scattering as arising predominately from the magnetic order and the  $\sigma\sigma$  from the antiferroquadrupolar order. The difference in the temperature dependence suggests that quadrupole ordering is driving the ordering of the magnetism. Furthermore, the widths, in reciprocal space, of the magnetic  $\sigma\pi$  scattering peaks are much greater than those of the antiferroquadrupole  $\sigma\sigma$  scattering peaks which also suggests that the antiferroquadrupole interactions frustrate the long range ordering of the magnetism in this system. This study exploited fully the unique combination of instrumental facilities available on XMaS (sub 4.2 K temperature, azimuthal scattering geometry, polarisation analysis, magnetic field, etc.). Further measurements are planned at XMaS on the study of this fascinating interplay of ordering in  $\text{TmGa}_3$ .



### Determination of the trace element content of healthy and cancerous breast tissue using XRF techniques

*M. J. Farquharson, K. Geraki, D. Bradley, A. Stunault - for further information contact: M.J.Farquharson, Department of Radiography, City University, London, EC1M 6PA (m.j.farquharson@city.ac.uk)*



A pilot experiment of 3 days duration was carried out on XMaS, in the single bunch mode, to test the feasibility of using synchrotron radiation to detect the presence of certain trace elements in breast tissue samples from their XRF spectra. It is believed that the concentration of these elements in tumours is different from that in healthy tissue. Some work had previously been attempted at City University using a laboratory x-ray source but the extremely low counting rates with such dilute systems results in very poor statistics.

The aim was to quantify the amounts of Fe, Cu and Zn present in the tissue samples, and to investigate, if possible, the presence of Ca and Rb. The samples were of two kinds, healthy tissue from breast reduction surgeries, and cancerous from biopsies or mastectomies. In total 21 samples of each kind were studied and these included 5 paired samples of cancerous and healthy tissues, each pair from one person. Water based calibration standards were prepared for Fe, Cu and Zn.

Samples and calibration standards were irradiated with a beam of energy tuned to 500eV above the K absorption edge for the element. This ensured a good fluorescence signal which can be separated from the scattered incident peak. The radiation emitted from the sample was recorded using a HPGe detector.

Figures (1) and (2) show the healthy and tumour response spectra for two incident energies, 7.6 keV and 10.2 keV for the detection of Fe and Zn

respectively Each spectrum was normalised with respect to the standards (using the scattered incident peak) in order to account for the different self-attenuation within each sample. In each spectrum the peak areas were determined and related to element concentrations (in ppm), using calibration curves obtained from measurements of known standard concentrations.

It was not possible to resolve two of the peaks of interest (K and Ca). This needs a Si detector and is one of the objectives for the next experiment.

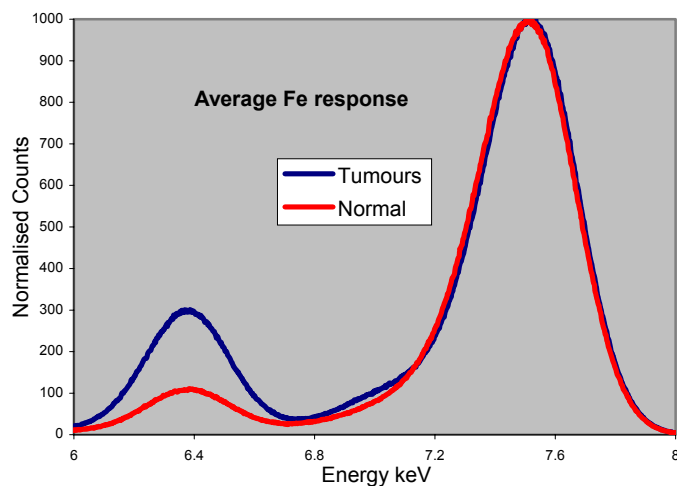


Figure (1): Mean healthy & tumour spectra for 7.6 keV

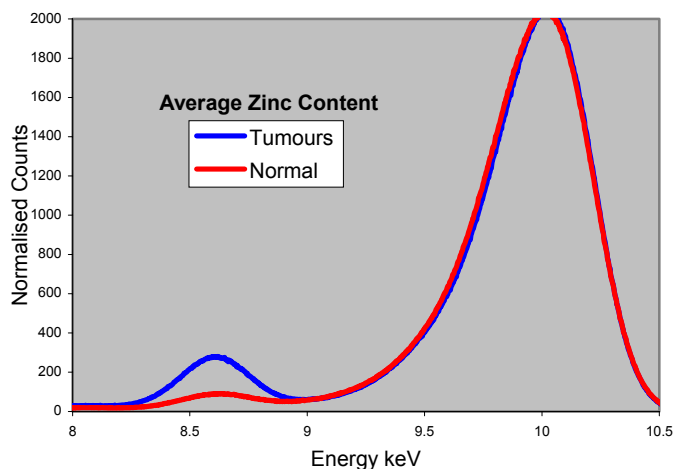


Figure (2): Mean healthy & tumour spectra for 10.2 keV

## Self assembly of nanoscale crystallites

*C. Nicklin, C. Norris, S. Alcock, M. Brust, S. Brown — for further information contact: C. Nicklin at the Department of Physics and Astronomy, Leicester University, University Road, Leicester LE1 7RH (cln@le.ac.uk)*

A grazing incidence small angle X-ray scattering (GISAXS) study was carried out at the XMaS beamline by collaborators from the Universities of Leicester, Birmingham and Liverpool. The samples are composed of gold nanoparticles (~4.5nm in diameter) surrounded by organic thiol-terminated molecules that self-assemble on the gold surface. As

a solution containing the clusters evaporates, the organic cage mediates a self-organising process whereby the clusters form close-packed ordered arrangements. The aim was to study the effect of external parameters, such as the sample temperature during evaporation, on the quality of the ordering. All results were from samples prepared from solvent evaporation on oxidised silicon (111) substrates.

The two sets of spectra were recorded from samples of particle assemblies, equivalent to 10 close packed cluster layers, over a range of preparation temperatures. All measurements were made at constant X-ray incidence angle and the detector scanning in the out-of-plane direction during vertical scattering and in-plane for horizontal scattering. The spectra clearly indicate that the horizontal scattering is unaffected by preparation temperature but large changes are exhibited in the vertical scans. At ~10°C there is significant peak narrowing and the appearance of further features at higher scattering angles. This indicates that cluster-layer stacking is improved at lower temperatures while the in-plane order remains unchanged. At lower temperatures splitting of the peaks reveals the presence of two important length scales in the vertical direction. Such results may be caused by diffusion-limited aggregation or by the presence of small domains which are disordered in the plane but well ordered in the layering direction. Further investigations, to include AFM measurements and additional GISAXS studies, are planned to study further this transition and also the effects of other external parameters (e.g. gas pressure).

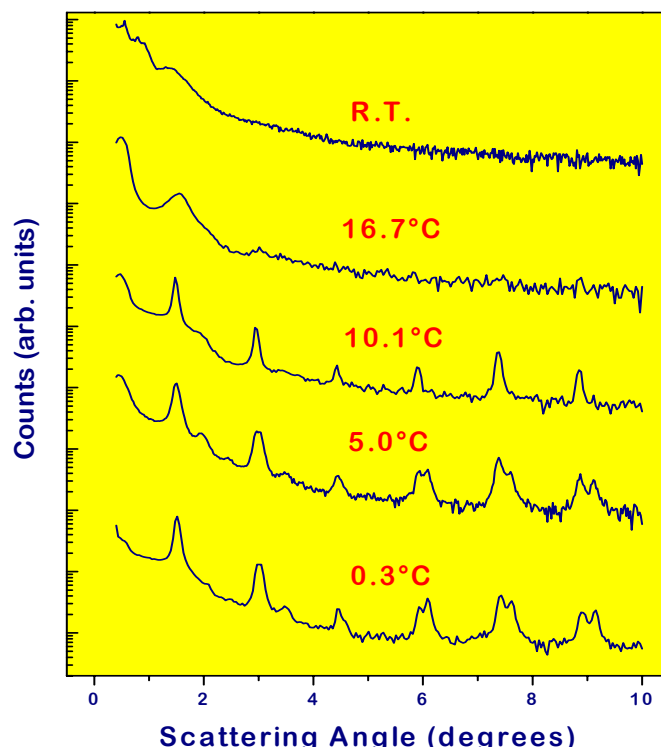


Figure 1: Vertical scattering of 4.5 nm particles. Temperature dependence.



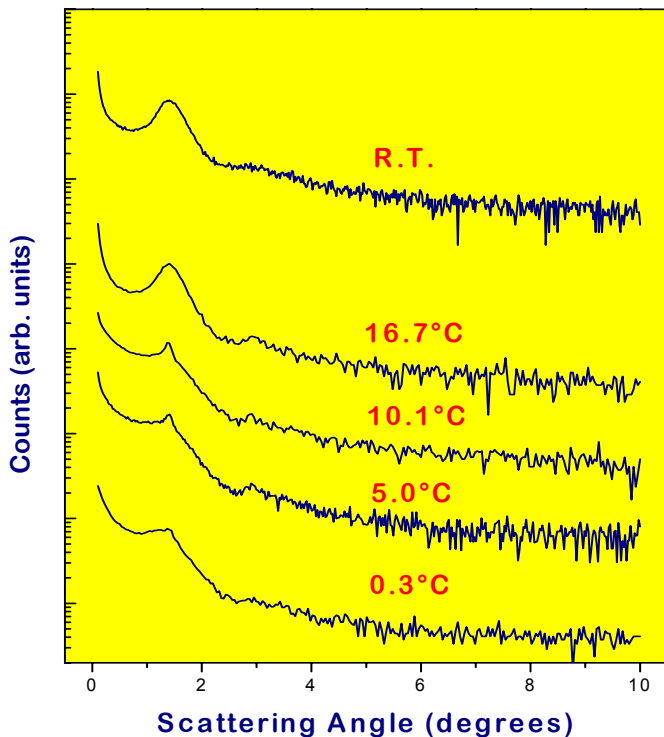


Figure 2: Horizontal scattering of 4.5 nm particles. Temperature dependence.

## X-ray reflection anomalous fine structure analysis of permalloy/copper multilayers

*T.P.A. Hase, B.D. Fulthorpe, J.D.R. Buchanan, G.M.Luo, B. K. Tanner - for further information contact Prof. B.K. Tanner at University of Durham, Department of Physics, South Road, Durham, DH1 3LE, U.K. (b.k.tanner@durham.ac.uk)*

X-ray Reflection Anomalous Fine Structure (RAFS) analysis has been used to study the changes in the layer density as well as the local chemical environment in sputtered permalloy/copper multilayers as a function of annealing temperature. Although similar to the more common Diffraction Anomalous Fine Structure (DAFS) technique, RAFS does not require high quality crystalline samples. Grazing incidence x-ray reflectivity measurements have been conducted as a function of incident x-ray photon energy. Fitting the smoothly varying part of the RAFS spectrum allows the density of the layers to be obtained uniquely. By analysing the intensity of the low angle Bragg peak, associated with the superlattice, as a function of energy (Figure 1) we have detected a strained permalloy layer at the permalloy/copper but not at the copper/permalloy interface. Upon annealing at 275°C the density difference between the copper and strained permalloy layers increases.

XAFS oscillations can also be extracted from the measured spectrum. A recurrent method is used to extract the real and imaginary components of the oscillations. A Fourier transformation on either of

the components then reveals the radial distribution function (Figure 2). On annealing, the nearest neighbour distance around Ni reduces but no change is observed around the Cu.

Similar measurements have also been performed on the diffuse scatter at an out-of-plane momentum transfer equal to the Bragg peak. As the diffuse scatter arises from the correlated component of the interface roughness, these oscillations provide a probe of the local environment of the interface atoms. For the NiFe/Cu (and also Co/Cu) multilayers examined, we found no differences in the local environment of the atoms at the interfaces from those in the body of the layers. An example of the oscillations around the Ni K edge is shown in Figure 3.

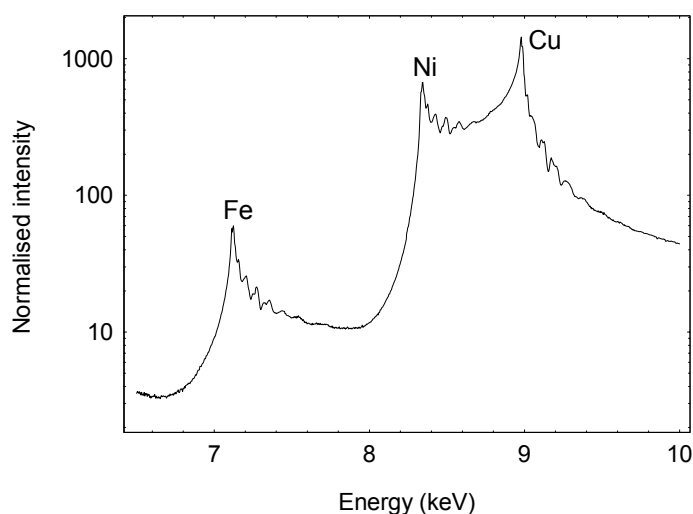


Figure 1: Bragg Peak intensity as a function of incident x-ray photon energy.

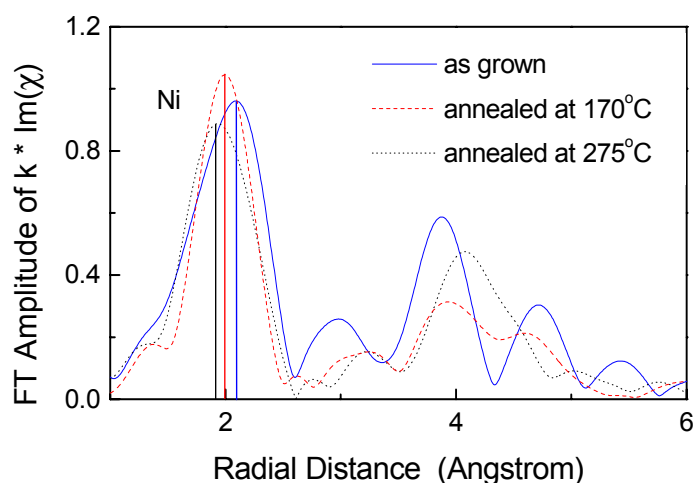


Figure 2: Radial distribution function calculated from the Fourier Transform of the imaginary component of the XAFS oscillations above the Ni K edge.

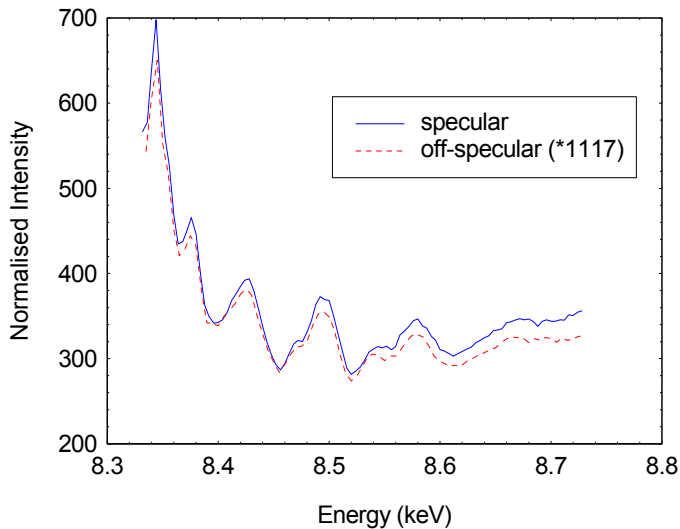


Figure 3: A comparison of the oscillations above the Ni edge from specular (line) and scaled diffuse (dashed) spectra.

## Performance of a diamond phase plate on the XMaS beamline

*L. Bouchenoire, M. J. Cooper, S. Brown, P Thompson - for further information contact L. Bouchenoire XMaS, BM28, ESRF, Grenoble boucheno@esrf.fr*

In ferromagnetic diffraction, the weak magnetic peaks are always superimposed on the much stronger charge peaks. The former can only be isolated from the latter by producing interference between charge and magnetic terms, for instance by using circularly polarised x-rays. One method is to reverse the direction of the sample magnetisation but this can only be done in soft ferromagnets and is plagued by sample movement due to the magnetic torques. The better alternative is to flip the helicity of the photons. Here we report on the operation of a phase plate installed on the XMaS beamline.

The 7.833keV incident linearly polarised radiation was converted into circular polarisation using a 0.78mm thick diamond crystal in Laue transmission. Figure 1 shows the possible values of  $P_c = \pm(1-P_1^2-P_2^2-P_{un}^2)^{1/2}$  deduced from our polarisation analyser data,  $P_{un}$  being the unpolarised component and  $P_1$  and  $P_2$  the stokes parameters. The correct sign of these data points (dotted line) is assigned from the modelled polarisation of the phase plate (red line) convoluted by a Gaussian function of width 1 arcsecs, representing the divergence of the beam. The diamond converted the 99.87% linear polarised incident beam to 99.85% circular polarised x-rays. The performance of the phase plate is illustrated by a XMCD signal measurement. A five micron GdCo<sub>2.5</sub> foil was mounted on the diffractometer at an angle of 45° to the incident beam and a 1 Tesla magnetic field applied parallel to the incident beam. Dichroism

measurements were undertaken at the Gd L<sub>3</sub> edge (7.243keV). The phase plate was used to flip the x-ray helicity. The applied field was held constant and the quarter-wave offset was changed from -77 to 77 arcsecs, which corresponds to  $P_c$  -99.61% and +99.63% respectively. The experiment was then repeated with the offset fixed at the same values, and the field flipped. The XMCD, defined as the difference in absorption ( $\mu^+ - \mu^-$ ), is comparable whether the field or the helicity are flipped (Figure 2) and is reproducible when the measurements are repeated on the other side of the Bragg condition (Figure 3). The dichroic signals are consistent and demonstrate the successful operation of the phase plate.

measurements were undertaken at the Gd L<sub>3</sub> edge (7.243keV). The phase plate was used to flip the x-ray helicity. The applied field was held constant and the quarter-wave offset was changed from -77 to 77 arcsecs, which corresponds to  $P_c$  -99.61% and +99.63% respectively. The experiment was then repeated with the offset fixed at the same values, and the field flipped. The XMCD, defined as the difference in absorption ( $\mu^+ - \mu^-$ ), is comparable whether the field or the helicity are flipped (Figure 2) and is reproducible when the measurements are repeated on the other side of the Bragg condition (Figure 3). The dichroic signals are consistent and demonstrate the successful operation of the phase plate.

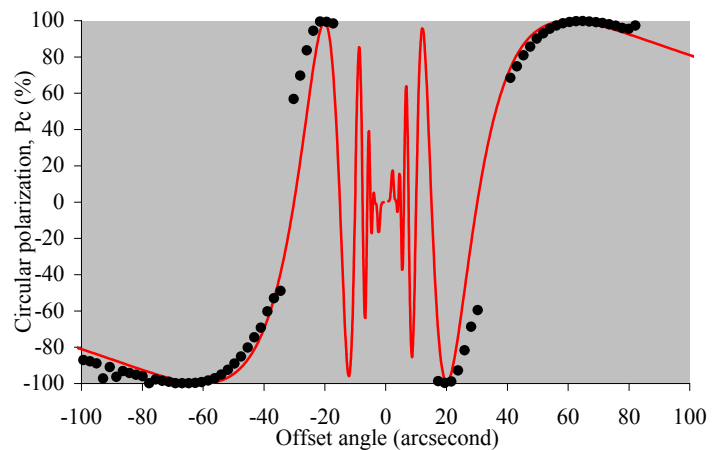


Figure 1: Circular Polarised X-rays,  $P_c = \pm(1-P_1^2-P_2^2-P_{un}^2)^{1/2}$ , measured at 7.833keV with a 0.78mm thick diamond crystal in Laue transmission (dotted line) in comparison with the theoretical values of  $P_c$  (red line).

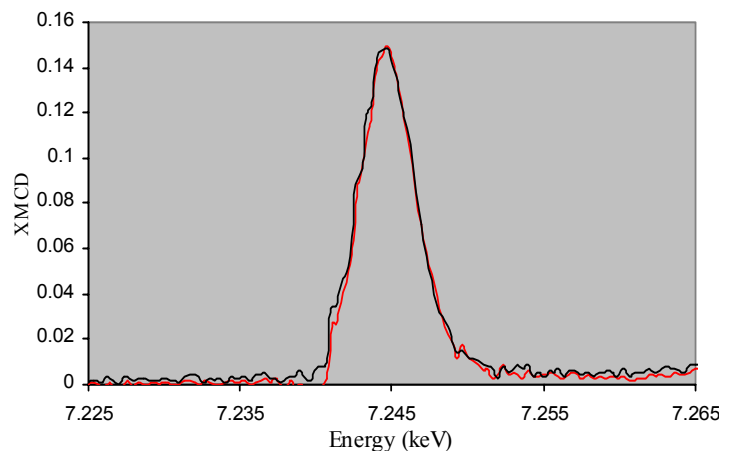


Figure 2: XMCD obtained by flipping the helicity (constant and positive magnetic field, red curve), and by flipping the field (+77 arcsecs offset angle, black curve).



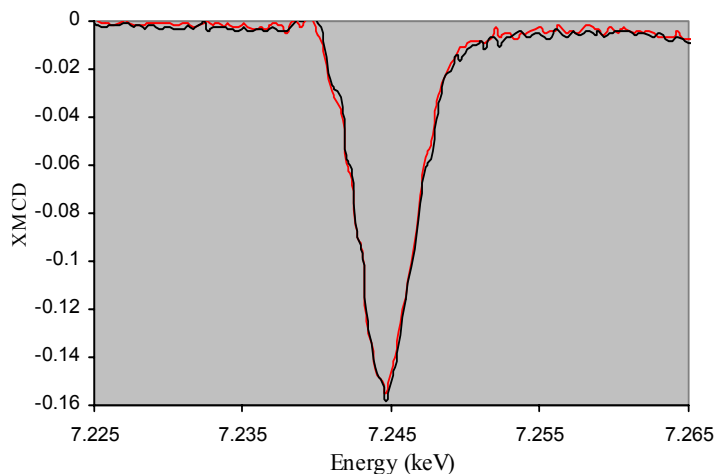


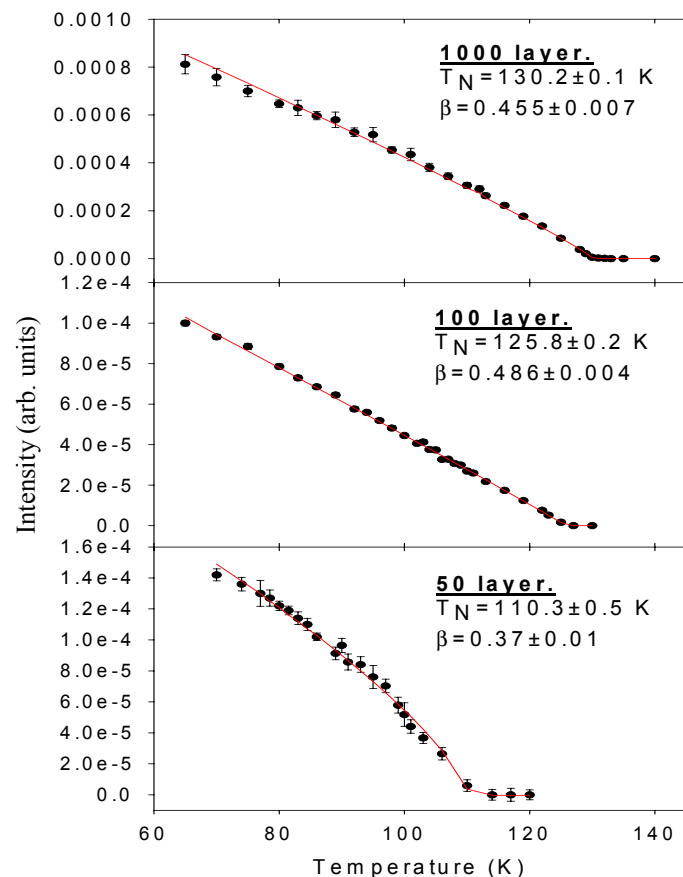
Figure 3: XMCD obtained by flipping the helicity (constant and negative magnetic field, red curve), and by flipping the field (-77 arcsecs offset angle, black curve).

## Resonant x-ray magnetic scattering in holmium thin films

A. D. F.Herring, W. J. Nuttall, J. P. Goff, M. F. Thomas, A. Stunault - for further information contact A. D. F.Herring at Department of Physics, University of Liverpool, Liverpool (herring@liv.ac.uk)

A number of very successful resonant x-ray magnetic scattering (RXMS) studies have been performed on bulk holmium making it an ideal choice for an investigation of the magnetic ordering at different film thicknesses, the purpose of this experiment.

Three MBE grown samples, having thicknesses of



280nm (1000 atomic layers), 28nm (100 layers) and 14nm (50 layers), were measured. The samples were capped with 10nm of yttrium and grown on 130nm Y and 90nm Nb seed and buffer layers. The (0,0,2-q) reflection was measured in each sample to investigate the effects of thickness on the range of the magnetic order.

The Néel temperature,  $T_N$ , decreases with decreasing sample thickness, as expected. The  $\beta$  value was found to be close to 0.5 for the 1000 and 100 layer samples but smaller for the 50 layer sample. Work is in progress to link these results to a strain effect in the thinnest sample.

## News round-up

The experimental reports in the previous pages are all as yet unpublished. Please email the contact person if you are interested in any of them or wish to quote these results elsewhere.

### Our web site

This is at:

[http://www.esrf.fr/exp\\_facilities/BM28/xmas.html](http://www.esrf.fr/exp_facilities/BM28/xmas.html)

It contains the definitive information about the beamline including experimental report forms and an on-line beamline manual.

### Living allowances

These remain at 350 Francs (53.3 Euros!) per day per beamline user—the equivalent actually paid in pounds sterling, of course. XMaS will continue to support up to 4 users per experiment if you can make a case for the presence of the fourth experimentalist. The ESRF hostel still appears adequate to accommodate all our users, though CRG users will always have a lower priority than the ESRF's own users. Do remember to complete the web-based “A form” requested of you when you receive the ESRF invitation, all attendees must be listed, since this informs the safety group of the attendees and is used to organise all site passes, meal cards and accommodation.

### Beamline people

There have been a few changes in the beamline staff since the last Newsletter. Here is a brief update:

**Project Co-ordinator** - David Paul, (dpaul@esrf.fr), is the person who can provide you with general information about the beamline, application procedures etc. There is now a **new procedure** in place for making such applications which is outlined on the last page of this newsletter. David should

normally be your first point of contact.

**Beamline Scientist(s)** - Anne Stunault left the team at the beginning of the year to become a beamline Scientist at IN14 at the ILL. We wish her well in her new post and extend our thanks for the very valuable and professional assistance she has given the beamline in her three years here. Following Anne's departure we are pleased to welcome to the team Danny Mannix who joined us from April 1st!

Danny has for the past 3 years been a post-doctoral researcher on ID20, "the other magnetic scattering beamline," and thus is an ideal new addition to the team.

Simon Brown (sbrown@esrf.fr) will continue to shoulder the main responsibility for helping the users, while Danny becomes familiar with the beamline, as well as maintaining/developing the scientific capability of the facility.

When you come to XMaS to perform an experiment either Simon or Danny will be selected as your "local contact" - and would be the first person to turn to for help.

**Technicians** - Paul Thompson (thompso@esrf.fr) continues to provide the day to day technical support for the beamline. John Kervin (jkervin@liv.ac.uk) who is based at Liverpool University provides further technical back-up and spends part of his time on-site at XMaS.

Matt Longfield (longfiel@esrf.fr) and Jon Wilmshurst (wilmshurs@esrf.fr) have both left the beamline—Matt is now a post doctoral researcher at ID20.

From October, 2000 we have a new PhD student, Laurence Bouchenoire (boucheno@esrf.fr), who is developing the phase plate to pursue studies of ferromagnets.

Malcolm Cooper (csmc@spec.warwick.ac.uk) and Chris Lucas (clucas@liv.ac.uk) continue to travel between the UK and France to oversee the operation of the beamline. The administration for XMaS is handled by Sandra Beaufoy at Warwick University (s.beaufoy@spec.warwick.ac.uk).

Bill Stirling - as you all know by now Bill became the Director General of the ESRF from 1<sup>st</sup> January 2001. Chris Lucas is now the Liverpool Co-Director.

### **The Peer Review Panel**

The membership of the panel has been changed recently and is now as follows:

Bob Cernik (*Chair*)

Bob Cywinski

Paul Fewster

Sean Langridge

Paul Strange (*replaces Julie Staunton*)

Nicholas Brookes (*replaces José Baruchel*)

John Hill

In addition either Malcolm Cooper or Chris Lucas attends their meetings.

### **PUBLISH PLEASE!!.....and keep us informed**

Papers reporting work on XMaS are beginning to appear. But now, more than ever, we need more of those publications to appear. We understand how this can take time but if we are to continue beyond the current 5-year contract we must demonstrate a reasonable output. We ask you to provide Sandra Beaufoy not only with the reference but also a preprint/reprint for our collection.

Over the next six months Malcolm Cooper and Chris Lucas will be talking to all the user groups in order to define the scientific programme which will underpin our application for a further 5 years of operation. Your assistance is vital and we hope to organise an autumn meeting to help refine the scientific case.

### **IMPORTANT!**

When beamline staff have made a significant contribution to your scientific investigation you may naturally want to include them as authors. Generally, though, we do ask that you add an acknowledgement, of the form:

"This work was performed on the EPSRC-funded XMaS beam line at the ESRF, directed by M.J. Cooper and C.A. Lucas/W.G. Stirling\*. We are grateful to the beam line team of S.D. Brown, D.F. Paul, A. Stunault/D. Mannix\* and P. Thompson for their invaluable assistance, and to S. Beaufoy and J. Kervin for additional support."

*\* as appropriate*

## Guidelines for Applying for Beam-time at the XMaS beamline

XMaS Pluo B3, ESRF, BP 220, 38043 Grenoble Cedex, France

Tel: +33 (0)4 76 88 24 36 Fax: +33 (0)4 76 88 24 55

web page : [http://www.esrf.fr/exp\\_facilities/BM28/xmas.html](http://www.esrf.fr/exp_facilities/BM28/xmas.html)

email: [dpaul@esrf.fr](mailto:dpaul@esrf.fr)

### Beamline Operation

The XMaS beamline at the ESRF, which came into operation in April 1998, has some 133 days of beam time available each year for UK user experiments, after deducting time allocated for ESRF users, machine dedicated runs and maintenance days. During the year, two long shut-downs of the ESRF are planned: 4 weeks in winter and 3 weeks in summer. At the ESRF beam is available for user experiments 24 hours a day.

### Applications for Beam Time

Two proposal review rounds are held each year, with deadlines for submission of applications, normally, the middle Friday of **April** and **October** for the scheduling periods August to February, and February to July, respectively. **Applications for Beam Time** are to be submitted **electronically** (the paper versions are no longer acceptable) following the successful model now used by the ESRF. Please consult the instructions given in the ESRF web page:

[www.esrf.fr](http://www.esrf.fr)

Follow the links: “**User Guide**”

And: “**Applying for Beam Time**”

Follow the instructions carefully for the electronic submission. A brief description of the process will also be included in the reminder that is emailed to our users shortly before the deadline—for any problems contact D. Paul.

Technical specifications of the Beamline and instrumentation available are described in the *XMaS* web page.

When preparing your application, please consider the following:

- All sections of the form must be filled in. Particular attention should be given to the safety aspects, and the name and characteristics of the substance completed carefully. Experimental conditions requiring special safety precautions such as the use of lasers, high pressure cells, dangerous substances, toxic substances and radioactive materials, must be clearly stated in the

proposal. Moreover, any ancillary equipment supplied by the user must conform with the appropriate French regulations. Further information may be obtained from the ESRF Experimental Safety Officer, tel: +33 (0)4 76 88 23 69; fax: +33 (0)4 76 88 24 18.

- Please indicate the dates that you would be unable to attend if invited for an experiment. This will help us to produce a schedule that is satisfactory for all.
- An experimental report on previous measurements must be submitted. New applications will not be considered unless a report on previous work is submitted. It is expected that these also, in the near future, will be submitted electronically, following the ESRF model. Reports must be submitted within 6 months of the experiment - paper versions should be sent to Sandra at Warwick. Forms for experimental reports are available from the XMaS web page – see above.
- The XMaS beamline is available for one third of its operational time to the ESRF’s user community. Applications for beamtime within that quota should be made by direct submission of the normal ESRF application form to the ESRF - **N. B., their deadlines are earlier than for XMaS! - 1st March and 1st September.** Applications for the same experiment may be made both to XMaS directly and to the ESRF. Obviously proposals successfully awarded beamtime by the ESRF will not then be given beamtime additionally in the XMaS allocation.

### Assessment of Applications

The Peer Review Panel for the UK-CRG considers the proposals, grades them according to scientific excellence, adjusts the requested beam time if required, and recommends proposals to be allocated beam time on the beamline.

Proposals which are allocated beam time must in addition meet ESRF safety and XMaS technical feasibility requirements.

Following each meeting of the Peer Review Panel, proposers will be informed of the decisions taken and some feedback provided.